catalysts

MDPI

Article

Valorisation of Corncob Residue towards the Sustainable Production of Glucuronic Acid

Wei Li [1,*], Shuguang Xu [2] and Xiang Xu [1,*]

[1] China National Chemical Engineering Third Construction Co., Ltd., Hefei 230601, China
[2] Department of Civil and Environmental Engineering, The Hong Kong Polytechnic University, Hung Hom, Kowloon, Hong Kong, China
* Correspondence: liwei2jinyang@126.com (W.L.); xxiang1970@163.com (X.X.)

Abstract: The production of glucuronic acid (GA) directly from actual biomass via chemocatalysis is of great significance to the effective valorisation of biomass for a sustainable future. Herein, we have developed a one-step strategy for the conversion of cellulose in corncob residue into GA with the cooperation of Au/CeO_2 and maleic acid, achieving a 60.3% yield. Experimental and density functional theory (DFT) results show that maleic acid is effective in the fractionation of cellulose from corncob residue and the depolymerisation of cellulose fragments to glucose, on account of the good capacity for proton migration. Au/CeO_2 is responsible for the selective oxidation of glucose to GA, in which the formation of glucaric acid is restrained, due to the weak capacity of Au/CeO_2 on the proton transfer without the occurrence of the ring-opening reaction of glucose. Therefore, the relay catalysis of Au/CeO_2 and maleic acid enables the production of GA via the complex cascade reactions. This work may provide insight regarding the conversion of actual biomass to targeted products.

Keywords: glucuronic acid; corncob residue; reaction mechanism

Citation: Li, W.; Xu, S.; Xu, X. Valorisation of Corncob Residue towards the Sustainable Production of Glucuronic Acid. *Catalysts* **2022**, *12*, 1603. https://doi.org/10.3390/catal12121603

Academic Editors: Qidong Hou and Da-Ming Gao

Received: 27 October 2022
Accepted: 3 December 2022
Published: 7 December 2022

1. Introduction

The rapid development of the economy and society depends on more renewable energy to supplement and replace fossil resources for a sustainable future [1–3]. Lignocellulosic biomass, a renewable and easily available resource abundant throughout the world, is being considered as a promising potential candidate [4–6]. Nowadays, lignocellulosic biomass and its derivatives are employed to produce various platform chemicals and fuels [7–9], which is regarded as an effective and industrially useful measure for biomass valorisation. Glucuronic acid (GA), a value-added chemical, has practical applications in pharmaceuticals, surfactants, and polymer synthesis. For instance, hyaluronic acid-based biodegradable polymer synthesised by GA is extensively used in biomedical engineering [10]. However, the high cost of GA has hindered the large-scale application of hyaluronic acid-based biodegradable polymers. There is a huge gap between the production capacity of GA and the output [11]. Therefore, it is important to develop economic strategies for GA production, such as using renewable lignocelluloses as feedstock.

Currently, commercial GA is produced by biochemical catalysis, generally using edible crops (glucose, sucrose, etc.) as the feedstock [12]. However, the use of edible crops would result in competition with human food production [13,14]. It is still a challenge to directly convert lignocelluloses to GA via biochemical catalysis due to the lack of enzymes with high activity. In addition, low productivity, the vulnerability and inseparability of microbes, and the process of wastewater treatment also hamper its large-scale production. A promising approach could be to improve chemocatalysis to achieve more sustainable technology for producing GA from lignocellulose. As reported, noble metal catalysts have been extensively employed for the production of GA via the oxidation of glucose. Therein, Au catalysts attract much attention due to their high and universal catalytic performance in the conversion of aldoses to their corresponding aldonic acids. For example,

the yield of GA could reach up to ~90% when Au is loaded on different metal oxide supports such as Al_2O_3, ZrO_2, and TiO_2 [15–17]. On the contrary, for the production of GA using non-noble metal catalytic systems, the yield is generally lower than 60% when using glucose, even in the presence of NaOH [18]. Although Au catalysts show outstanding catalytic performance on the conversion of glucose to GA, it is unsatisfactory for the conversion of actual lignocellulosic biomass due to the complex structure and interactions [19]. The synthesis of GA from cellulose is reported to achieve a yield of 60% over $Au/Cs_{1.2}H_{1.8}PW_{12}O_{40}$ catalysts but needs a lengthy reaction time (11 h) at 145 °C. Therein, $Cs_{1.2}H_{1.8}PW_{12}O_{40}$ is responsible for the hydrolysis of cellulose to glucose; the oxidation of glucose is promoted by Au nanoparticles. Such a tandem reaction could weaken the catalytic activity of the Au catalyst for cellulose. Unfortunately, only limited studies are have reported on the conversion of raw biomass for GA production. In the available literature, the yield of GA directly from actual lignocelluloses is shown to be considerably lower than those including cellulose [20].

In this work, we report the on production of GA directly from actual lignocelluloses via the conversion of the cellulose components by a synergic catalytic system (maleic acid and Au/CeO_2), achieving a good yield of GA (~60%, based on the amount of cellulose in the corncob residue, the contents of which are 17.2 wt% of lignin, 62.4 wt% of cellulose, 0.1 wt% of hemicellulose, 4.5 wt% of ash, and 15.8 wt% of others unknown) in the base free condition using O_2 as an oxidant, with the remaining lignin being usable for further processing. Therein, maleic acid is mainly used for the fractionation of corncob residue to obtain glucose; the transformation of glucose to GA is mainly catalysed by Au/CeO_2. We have also investigated the reaction mechanism by combining our experiment with that of the DFT study, which provides a comprehensive understanding of the role of maleic acid in the fractionation of corncob residue to glucose.

2. Results and Discussion

2.1. The Characterization of the Au/CeO_2 Catalyst

The prepared Au/CeO_2 catalysts are first characterized with different Au loadings. The XRD patterns (Figure 1) show that the peaks at $2\theta = 36.2°$, corresponding to the (111) lattice plane of Au^0, and the calculated particle size is found to gradually increase with the increasing of Au content. The peaks at $2\theta = 28.5°$, 33.1°, 47.5°, 56.3°, and 59.1° correspond to the lattice planes of CeO_2. This demonstrated the presence of cubic phases Au (PDF 04-0784) and CeO_2 (PDF 43-1002) in the prepared Au/CeO_2 catalysts. XPS analysis shows two obvious peaks with the binding energy centred at 87.4 and 83.7 eV, which correspond to the core levels of Au 4f5/2 and 4f7/2, respectively, further confirming the existence of Au^0 in the catalyst [21]. SEM images show that Au nanoparticles spread evenly over the surface of the CeO_2 (Figure S1), and the transmission electron microscopy (TEM) analysis reveals Au particles with a spherical structure on CeO_2 surface (Figure 1). ICP-AES analysis demonstrated that the actual loadings of Au in the catalyst are almost equal to the expected amounts (Table S1). N_2 adsorption—desorption isotherm analysis shows that the prepared Au/CeO_2 catalysts are mainly in a mesoporous state (Figure S1). In addition, the BET surface area is found to be almost unchanged by the increasing Au loading (Table S1), which excludes the variation of catalytic activity derived from the change of the specific surface.

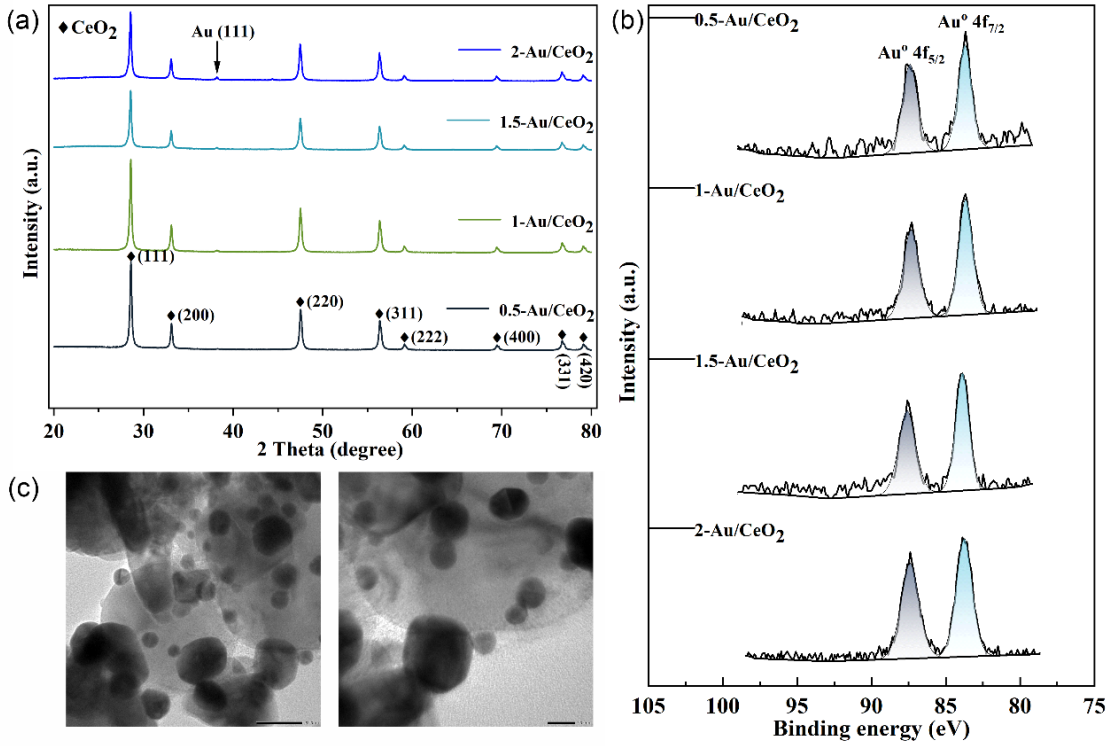

Figure 1. The characterizations of the prepared Au/CeO_2 catalysts. (**a**) The XRD patterns of the catalysts. (**b**) The XPS analysis of the prepared Au/CeO_2 catalyst. (**c**) The TEM image of Au/CeO_2 catalyst.

2.2. The Direct Conversion of Cellulose in Corncob Residue to GA

To effectively promote the tandem reaction in the conversion of corncob residue to GA, including the fractionation of cellulose to glucose and glucose oxidation, the cooperation of acid and Au/CeO_2 is applied. It is reported that dicarboxylic acids are effective in the hydrolysis of cellulose/hemicellulose with high carbon utilization [22–24]. Therefore, the cooperative effect of Au/CeO_2 and four typical dicarboxylic acids (maleic acid, malic acid, citric acid, and tartaric acid) are investigated for the conversion of corncob residue, and the results are shown in Table 1. It is found that the catalytic activity from maleic acid is higher than from others; the yield of GA could reach 56.0%, and the conversion of cellulose in corncob residue is ~100% with the presence of O_2. For comparison, the yield of GA from a single maleic acid and Au/CeO_2 is less than 10%, with the cellulose conversion being less than 50% (Table S2). This finding proves the synergistic effect between maleic acid and Au/CeO_2. In addition, several by-products including formic acid, glycolic acid, glucaric acid, and glyceric acid are also obtained, but with low yields (Table 1). In addition, Au/CeO_2 catalysts also show better catalytic activity than some typical Au-based catalysts, which focus on the conversion of glucose to GA, such as Au/Al_2O_3, Au/ZrO_2, and Au/TiO_2 (Table S3). We further optimized reaction conditions, including the amount of maleic acid and Au/CeO_2, the pressure of O_2, and the reaction time and temperature (Tables S4–S8). It is found that under the optimal conditions (0.2 g Au/CeO_2, 6 mM maleic acid, 443 K, 1.0 MPa O_2, and 1.5 h), the yield of GA can reach 60.3%, and the corresponding concentration is 6.8 mg/mL. Additionally, about 0.221 g of solid residue is obtained after the reaction. If all the residue is lignin, the calculated conversion of lignin is 7.5% due to the original lignin being 0.239 g. After the reaction, XPS and TEM analyses (Figure S2) of the spent catalyst showed that the main component was still the Au^0 species, which proved that the Au^0 species in the Au/CeO_2 catalyst is stable during the conversion of corncob residue. However, according to the TEM analysis, the aggregation of gold particles is observed after the reaction.

Table 1. The catalytic activity of the cooperation of four typical dicarboxylic acids and Au/CeO_2 on the conversion of corncob residue to GA [a].

	Cellulose Conversion (%)	Yield of Products (%)				
		GA	Glucaric Acid	Formic Acid	Glycolic Acid	Glyceric Acid
Maleic acid	~100	56.0	0.3	3.4	0.6	1.3
Malic acid	~100	51.1	0.5	4.2	0.9	1.7
Citric acid	54	13.4	0.1	1.7	0.3	2.5
Tartaric acid	85	40.7	0.3	3.9	0.8	1.1

[a] Reaction conditions: 1.0 g corncob residue; 0.1 g Au/CeO_2; 5 mM dicarboxylic acids; 50 mL H_2O; O_2, 1 MPa; temperature, 443 K; time, 2.0 h.

2.3. The Role of Maleic Acid and Au/CeO$_2$ on the Selective Conversion of Corncob Residue

2.3.1. Fractionation of Cellulose from Corncob Residue

The substantial interlinkages among raw lignocelluloses seriously impede further degradation of targeted chemicals, in which fractionation is the effective measure to separate the main components to benefit from their valorisation [25]. Therefore, we have investigated the role of maleic acid and Au/CeO_2 on the fractionation of corncob residue (Table S2). It is found that in the case of maleic acid, no cellulose is tested in the reaction residue, which is similar to the results regarding the cooperation of maleic acid and Au/CeO_2. On the contrary, when only Au/CeO_2 is used, 92% cellulose remains in the reaction residue, meaning that Au/CeO_2 shows a limited effect on the fractionation. It is proved that in the maleic acid and Au/CeO_2 catalytic system, maleic acid is responsible for the fractionation of cellulose from corncob residue. We then investigated the performance of maleic acid on the fractionation of cellulose through the analysis of cellulose components' removal at various temperatures based on the decreasing amount of cellulose in solid residue. As shown in Figure 2, the removal of cellulose sharply increased with the increasing reaction temperature and was almost removed at 433 K. The raw material and solid residues are characterized by FTIR spectroscopy. It is found that the characteristic peak assigned to cellulose (1320 cm^{-1}) decreases gradually with the increase of reaction temperature and almost disappears at 433 K. In this regard, the characteristic peak assigned to lignin (1512 cm^{-1}) continues to exist [26], which suggests that the remaining solid residue is possibly the unconverted lignin that may be used for further transformation.

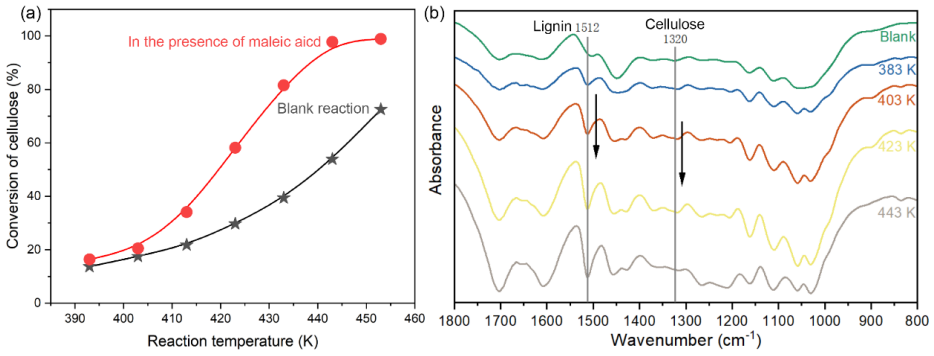

Figure 2. The performance of maleic acid on the fractionation of cellulose from corncob residue. (**a**) The conversion of cellulose; (**b**) FTIR spectra of solid samples after reaction at the different reaction temperatures.

To obtain deeper insight into the performance of maleic acid for the cleavage of intra-/inter-chain hydrogen bonds which dominated the fractionation of cellulose, we conducted the DFT study employing cellobiose as model units of cellulose, respectively (Figure 3). As calculated, after the introduction of maleic acid, the new intra-chain and inter-chain

hydrogen bonds from maleic acid are more stable than those of the original hydrogen bonds (the original hydrogen bonds are substituted by the new), and the stabilization energy (which is calculated by the diffidence of the H-bonds energy between the initial one and the one after maleic acid introduction) is 3.2 and 4.7 kcal mol^{-1}, respectively. Thus, maleic acid is successfully employed for the breaking of intra-chain and inter-chain hydrogen bonds in corncob residue due to the higher interaction energy to promote the fractionation of cellulose. It is proven that the intra-/inter-chain hydrogen bonds could be broken by the introduction of maleic acid to form the new hydrogen bonds between maleic acid and cellobiose. This would sever the connection of chains to realize the fractionation, thus becoming the cellulose fragments. These results are consistent with the present experimental results and also with those in the literature [25].

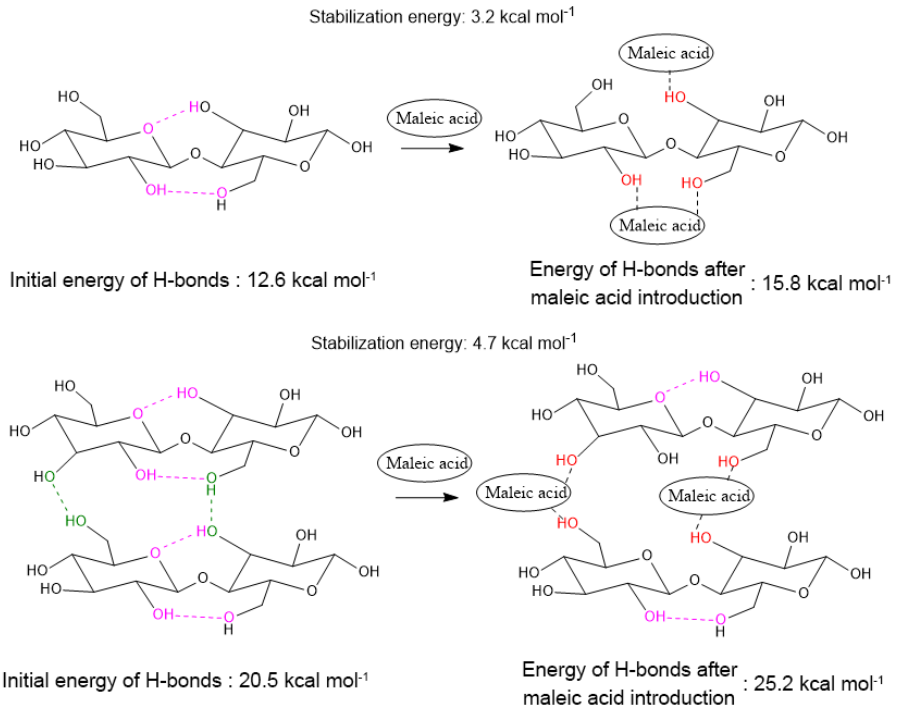

Figure 3. The performance of maleic acid on the breaking of inter- and intra-chain hydrogen bonds in cellobiose.

2.3.2. Depolymerisation of Polysaccharide to Glucose

After the fractionation, the cellulose fragments must be further transformed to glucose, which is due to the higher reactivity of glucose than of cellulose fragments [27,28]. In our study, we find that within 1.5 h at 423 K, the amount of glucose increased before 45 min, and is then gradually consumed as the reaction continues. At that time, the yield of GA is sharply increased to ~50% (Figure S3), which shows the typical feature of the reaction intermediate and validates the intermediate of glucose in the conversion of corncob residue to GA. In that case, we have investigated the role of maleic acid and Au/CeO_2 on the depolymerisation using cellulose as the model chemical, and the results are shown in Table S9. In the presence of Au/CeO_2, only a 14% conversion of cellulose is observed. In comparison, an approximate 100% conversion of cellulose would occur in the presence of maleic acid, which is close to that from the cooperation of maleic acid and Au/CeO_2, and is much higher than that from Au/CeO_2. In addition, we have also conducted a GPC analysis of the reaction solutions from the three cases mentioned. As seen in Figure 4, the Mw from the catalysis of Au/CeO_2 is mainly concentrated in the range of 2000 to 10,000 Da, which is 52% for the oligosaccharides without sufficient depolymerisation. In addition, the Mw < 200 Da is less than 8%, which proved the weak depolymerisation capacity of Au/CeO_2. However, in the presence of maleic acid with/without Au/CeO_2,

in addition to the Mw < 200 Da being more than 45%, the Mw > 2000 Da is less than 10%, which indicates that deep depolymerisation happens on the cellulose, mainly being converted to monosaccharides (Mw < 200 Da) or oligosaccharides with a low degree of polymerisation (Mw > 2000 Da). We have also supplemented the GPC analysis of the reaction solution from corncob residue. The results are similar to those from cellulose, which are shown below. It is found that the M_w from the catalysis of Au/CeO_2 is also mainly concentrated in the range of 2000 to 10,000 Da, which is 69% for the oligosaccharides without sufficient depolymerisation. In addition, the Mw < 200 Da is less than 5%. It is evident that compared to cellulose as the feedstock, corncob residue is more difficult to transform in the presence of Au/CeO_2. When maleic acid is introduced with/without Au/CeO_2, monomers (Mw < 200 Da) and oligomers (2000 Da > Mw > 200 Da) are also obviously increased to 39% and ~50%, respectively, and long-chain component (Mw > 2000) Da is converted, the percentage of which being reduced to less than 10%. Therefore, it is clear that maleic acid, rather than Au/CeO_2, is mainly responsible for the depolymerisation of cellulose to glucose.

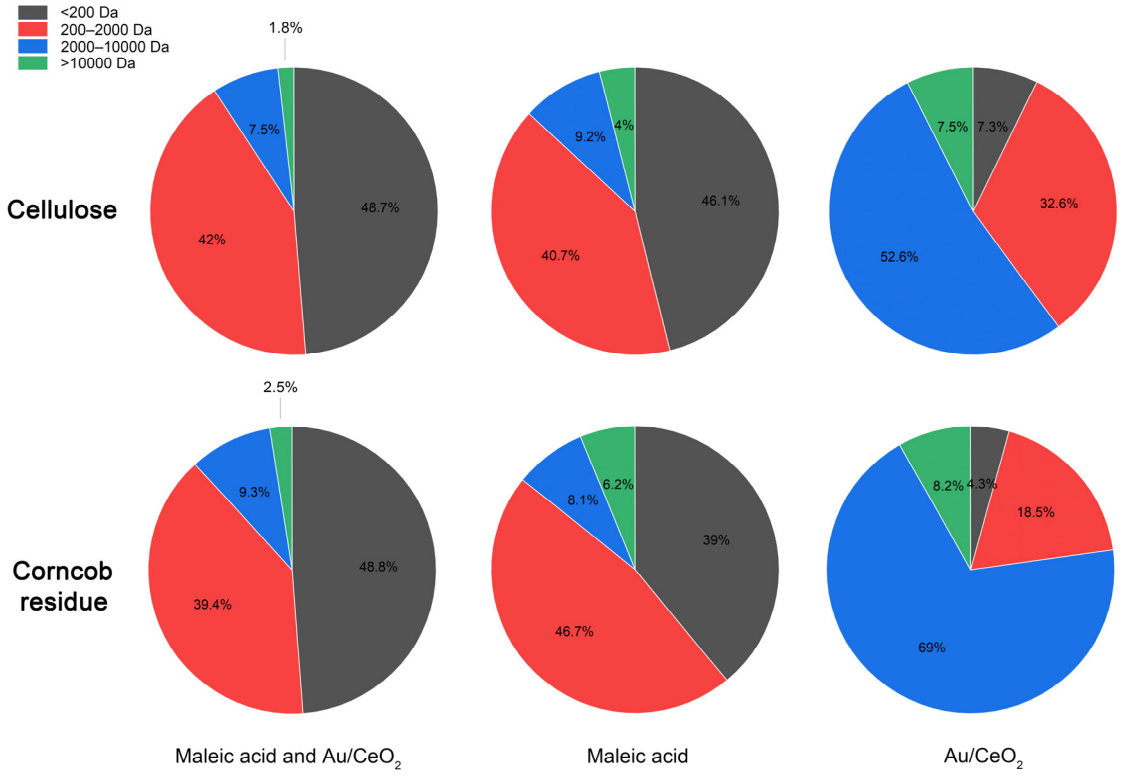

Figure 4. GPC analysis of the liquid products at different reaction conditions from cellulose and corncob residue.

We then conducted the DFT study for the investigation of cellulose depolymerisation to glucose, in which the 1,4-glycoside bond-breakage is considered the key step. Therefore, cellobiose with the typical 1,4-glycoside bond is employed as model compounds of cellulose (Figure 5). It is calculated that in the absence of maleic acid (the blank reaction), water could be the proton donator for the breaking of the 1,4-glycoside bond by the H-shift from water to O in the 1,4-glycoside bond. Meanwhile, the remaining OH from water could shift to the C2, realizing the depolymerisation of cellobiose to form two glucose with an energy barrier of 45.9 kcal mol^{-1}. On the contrary, when maleic acid is introduced, the proton is transferred from -COOH of maleic acid to O in the 1,4-glycoside bond, creating a maleate with one -COO- and one -COOH. The protonation of the 1,4-glycoside bond promotes the breaking of this bond with a 13.9 kcal mol^{-1} energy barrier to form one glucose and one dehydroxylated glucose. Thereafter, water could provide OH to the dehydroxylated

glucose, which reforms the other glucose, and the remaining H shifts to the maleate to obtain maleic acid. The catalytic cycle for the depolymerisation of cellobiose to glucose is completed with maleic acid as the catalyst. In that case, the energy barrier (13.9 kcal mol^{-1}) from maleic acid is much lower than that from the blank reaction (45.9 kcal mol^{-1}), proving that maleic acid is responsible for the depolymerisation of polysaccharide, which accords with the experimental results. Additionally, we deduce that maleic acid, due to the Lewis acidity, is beneficial for the conversion of polysaccharides to glucose. In addition, as the dicarboxylic acid, maleic acid has a good capacity to store protons for its releasing or accepting, which is much stronger for the H-shift than water. Therefore, the energy barrier from the catalysis of maleic acid is much lower than that directly from the water.

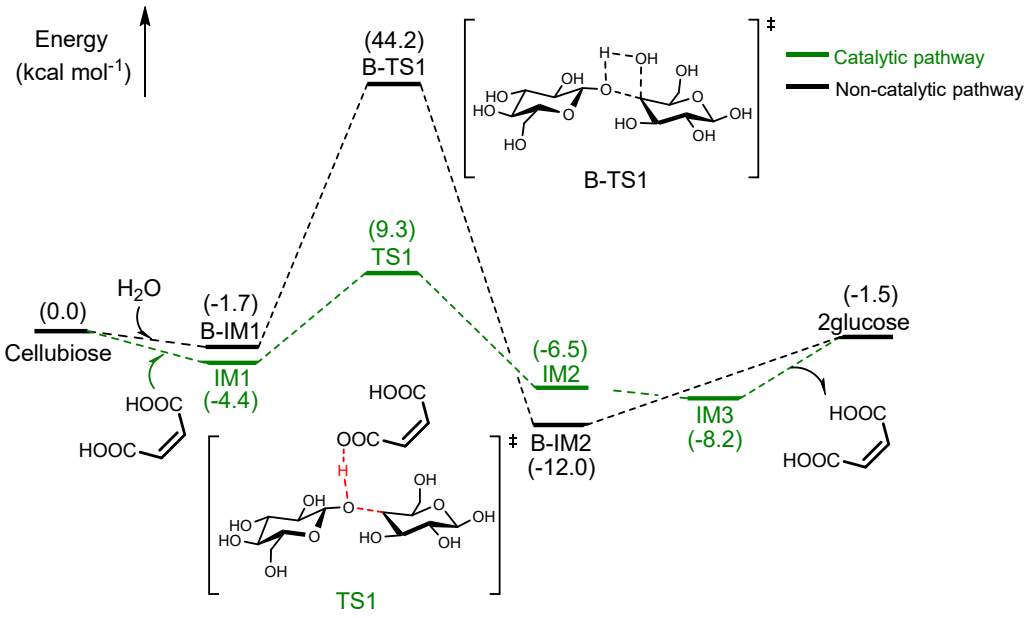

Figure 5. The energy profiles (in kcal mol^{-1}) and the optimized geometries for the hydrolysis of cellobiose in catalytic/non-catalytic pathways.

2.3.3. Oxidation of Glucose to GA

To elucidate the key impacts of the Au/CeO_2-maleic acid catalytic system on the oxidation of glucose to GA, glucose is employed as the starting material for several control experiments. As shown in Table S10, in the presence of maleic acid, the GA yield is 75% with a ~100% conversion of glucose, which is similar to that from the catalysis of Au/CeO_2 and maleic acid. In comparison, no GA is observed when a single maleic acid is used for glucose conversion. Furthermore, deep oxidation could be the popular by-product of glucose oxidation, although the amount of which was very limited in our study. It is therefore evident that Au/CeO_2 is mainly responsible for the selective oxidation of glucose to GA. In addition, we have also explored the significant role of O_2 in glucose conversion (Table S11). However, only 12% GA is obtained from glucose in the presence of N_2 with the same pressure of O_2, in which case 5-hydroxymethylfurfural becomes the main product, with a yield of 18%. Thus, O_2 could be the oxidizing agent during the conversion of glucose to GA.

To clarify the influence of Au/CeO_2 and O_2 on the conversion of glucose selectively to GA, and specifically the mechanism for avoiding the formation of glucaric acid, the DFT study was conducted for its insight at the molecular level. As proved by XRD results of the Au/CeO_2 catalyst, it was found that Au(111) is the main exposed crystal of the Au/CeO_2 catalyst, which is therefore selected as the calculation model. In this regard, two reaction pathways for the oxidation of glucose to GA are taken into consideration. One (Figure 6) is the direct oxidation of -C(6)H_2OH to -COOH (Path A). At the beginning of the reaction, glucose is adsorbed on Au(111) by the interaction of O in C6 and Au, and with O_2 as the

oxidative agent, nearby glucose is also adsorbed on Au(111) by the interaction of O and Au, for which the absorption energy is −11.2 kcal mol^{-1}. It is calculated that H in C6 could be removed by the absorbed O_2, forming *OOH, the energy barrier of which is 24.6 kcal mol^{-1}. The remaining H in C6-O is then removed by *OOH with an 18.0 kcal mol^{-1} energy barrier, realizing the oxidation of -CH_2OH to -CHO in C6. Subsequently, H in -CHO of C6 is converted to be -COOH of C6, which undergoes the migration of H in -CHO to O_2 to obtain -CO* of C6 and *OOH, and the *OH from *OOH shifts to -CO* of C6, leading to the formation of GA. The energy barriers of those two steps are 25.1 and 17.3 kcal mol^{-1}, respectively. Therefore, the activation of C-H in -CHO with the highest energy barrier is the rate-controlling step. As a comparison, another reaction pathway (Figure 6) for the generation GA involving the oxidation of -C(1)HO to -COOH and -C(6)H_2OH to -CHO was also taken into account (Path B). It was calculated that before the oxidation of –C(1)HO to -COOH, the ring-opening of cycle-glucose to chain-glucose is necessary, which is realized by the H in -C(1)-OH migrating to C(5)-O with a 35.2 kcal mol^{-1} energy barrier to induce the breaking of C1-O. Such an energy barrier is much higher than those mentioned in the literature that used oxygen (hydroxy)-containing catalysts such as Cu_2O [29] and $[Y(OH)_2(H_2O)_2]^+$ [30], and $Mg(OH)^+$ [31] for the cycle-opening of glucose. This difference is mainly on account of the promotion of H-migration by oxygen (hydroxy)-containing groups. After the chain-glucose formation, –CHO would be oxidized to -COOH via the H removal from -CHO to O_2, and the resulting -CO* is combined with *OOH to form *OH. The energy barriers for those two steps are 22.7 and 16.9 kcal mol^{-1}, respectively. Furthermore, the oxidation of -C(6)H_2OH to -CHO also involves similar steps, including -C(6)-H activation (26.9 kcal mol^{-1} energy barrier) and H-migration from -OH in C(6) to *OOH (19.4 kcal mol^{-1} energy barrier). In this regard, the ring-opening with the highest energy barrier is the rate-controlling step. It is found that the highest energy barrier for Path A is lower than that for Path B (25.1 vs. 35.2 kcal mol^{-1}), which indicates the kinetic advantage of Path A, avoiding the ring-opening of cycle-glucose. Importantly, due to the inevitable occurrence of the ring-opening of cycle-glucose, glucaric acid is generally formed as the by-product during glucose conversion [17,18]. In our work, Path A involves the oxidation of glucose to GA without ring-opening and is more favourable than Path B. Therefore, the formation of glucaric acid is restrained by the limitation of ring-opening, which is mainly due to the weak capacity of Au/CeO_2 on the proton transfer.

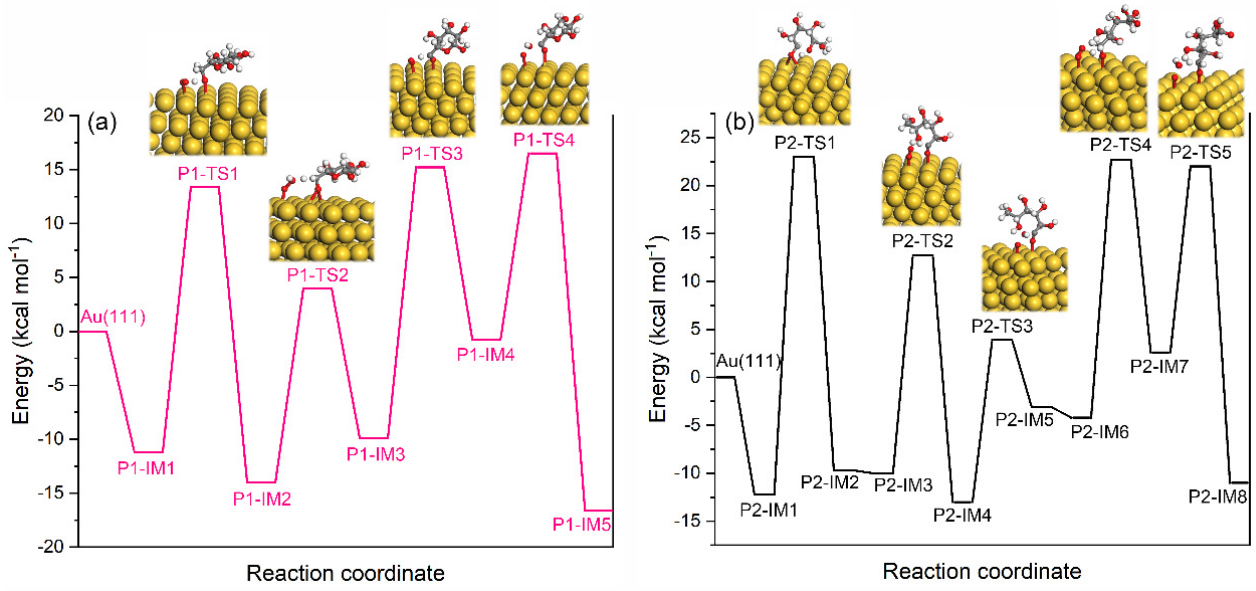

Figure 6. The energy profiles (in kcal mol^{-1}) and the optimized geometries for the conversion of glucose to GA from two reaction pathways catalysed by Au/CeO_2. (**a**) the generation GA involving the direct oxidation of -C(6)H_2OH to -COOH; (**b**) the generation GA involving the oxidation of -C(1)HO to -COOH and -C(6)H_2OH to -CHO.

3. Experimental Section

3.1. Catalyst Preparation

Au/CeO_2 catalyst was prepared using the deposition—precipitation (DP) method, according to the literature [21]. Typically, 0.04 g chloroauric acid was mixed with the suspension of 2.0 g CeO_2. The pH was then adjusted to 9.0 by adding 0.25 M ammonia. After stirring for 6 h at room temperature, the sample was washed using deionized water and then separated by filtration. The resulting precipitate was dried at 80 °C for 1 h in an oven, and then pre-reduced in 5% H_2/Ar for 2 h at 350 °C.

3.2. Catalytic Reaction

Corncob residue was added to a 100 mL stainless steel autoclave reactor equipped with a temperature controller and a magnetic stirring device. A total of 1 g of corncob residue powder and 50 mL of deionized water were mixed with the designated amount of maleic acid in the reactor. The interior air was completely replaced with high-purity nitrogen (99.99%) for 3 min, and the initial pressure in the reactor was increased to 2.0 MPa with nitrogen. The reactor was heated to the designated temperature by the equipped electric heating sleeve after about 30 min, (usually 433 K) with a stirring rate of 400 rpm for a certain time (usually 1.5 h). When the reaction was finished, the reactor was quenched to room temperature with an ice water mixture after about 15 min. The separated liquid products after filtration were subjected to qualitative and quantitative analyses. The standard errors were computed for each point. The standard deviations were less than 5%.

4. Conclusions

In summary, a one-step strategy is used for the production of GA directly from the renewable corncob residue, and the yield of GA could reach up to 60.3% based on the cellulose. Experimental and calculational results show that the significance of Au/CeO_2 and maleic acid co-contribute to realize the complex reaction on the selective formation of GA. It is revealed that the three procedures include the fractionation of corncob residue, depolymerisation of cellulose to glucose, and the oxidation of glucose to GA. Therein, maleic acid would promote the first two procedures due to its acidity and enable the formation of glucose; subsequently, glucose would be oxidated to GA by Au/CeO_2, avoiding the deep oxidation of GA to glucaric acid, in which O_2 is the oxidizing agent.

Supplementary Materials: The following supporting information can be downloaded at: https://www.mdpi.com/article/10.3390/catal12121603/s1, Materials; Product analysis (Figure S4); Quantum chemical computational details [32–41]; Figure S1: N_2 adsorption-desorption isotherm for the catalysts; Figure S2: The characterizations of the spent Au/CeO_2 catalysts. (a) The XPS analysis of the prepared Au/CeO_2 catalyst. (b) The TEM image of Au/CeO_2 catalyst; Figure S3: The time course of the glucose and GA formation during the conversion of corncob residue at 423 K; Figure S4: The HPLC analysis of the mixture of gluconic acid and glucuronic acid; Table S1: Textural properties of the catalysts; Table S2: The control experiments on the conversion of corncob residue to GA [a]; Table S3: The catalytic activity of different Au-based catalysts on the conversion of corncob residue to GA [a]; Table S4: The effect of the amount of maleic acid on the conversion of corncob residue to GA [a]; Table S5: The effect of the amount of Au/CeO_2 on the conversion of corncob residue to GA [a]; Table S6: The effect of the amount of O_2 pressure on the conversion of corncob residue to GA [a]; Table S7: The effect of reaction temperature on the conversion of corncob residue to GA [a]; Table S8: The effect of reaction time on the conversion of corncob residue to GA [a]; Table S9: The control experiments on the conversion of cellulose to GA [a]; Table S10: The control experiments on the conversion of glucose to GA [a]; Table S11: The control experiments on the conversion of glucose to GA at different atmosphere [a].

Author Contributions: Conceptualization, X.X.; methodology, S.X.; software, W.L.; validation, W.L., S.X. and X.X.; formal analysis, W.L.; investigation, W.L.; resources, W.L. and X.X.; data curation, W.L.; writing—original draft preparation, W.L.; writing—review and editing, W.L. and X.X.; visualization, W.L.; supervision, X.X.; project administration, X.X. All authors have read and agreed to the published version of the manuscript.

Funding: This research received no external funding.

Data Availability Statement: Data is contained within the article or Supplementary Material.

Conflicts of Interest: The authors declare no conflict of interest.

References

1. Sudarsanam, P.; Peeters, E.; Makshina, E.V.; Parvulescu, V.I.; Sels, B.F. Advances in porous and nanoscale catalysts for viable biomass conversion. *Chem. Soc. Rev.* **2019**, *48*, 2366–2421. [CrossRef]
2. Zhu, Y.; Romain, C.; Williams, C.K. Sustainable polymers from renewable resources. *Nature* **2016**, *540*, 354–362. [CrossRef] [PubMed]
3. Besson, M.; Gallezot, P.; Pinel, C. Conversion of biomass into chemicals over metal catalysts. *Chem. Rev.* **2014**, *114*, 1827–1870. [CrossRef] [PubMed]
4. Li, Z.; Ji, S.; Liu, Y.; Cao, X.; Tian, S.; Chen, Y.; Niu, Z.; Li, Y. Well-Defined Materials for Heterogeneous Catalysis: From Nanoparticles to Isolated Single-Atom Sites. *Chem. Rev.* **2020**, *120*, 623–682. [CrossRef] [PubMed]
5. Mika, L.T.; Csefalvay, E.; Nemeth, A. Catalytic Conversion of Carbohydrates to Initial Platform Chemicals: Chemistry and Sustainability. *Chem. Rev.* **2018**, *118*, 505–613. [CrossRef]
6. Zhang, Z.; Song, J.; Han, B. Catalytic Transformation of Lignocellulose into Chemicals and Fuel Products in Ionic Liquids. *Chem. Rev.* **2017**, *117*, 6834–6880. [CrossRef]
7. Zhang, Z.; Huber, G.W. Catalytic oxidation of carbohydrates into organic acids and furan chemicals. *Chem. Soc. Rev.* **2018**, *47*, 1351–1390. [CrossRef]
8. Sudarsanam, P.; Zhong, R.; Van den Bosch, S.; Coman, S.M.; Parvulescu, V.I.; Sels, B.F. Functionalised heterogeneous catalysts for sustainable biomass valorisation. *Chem. Soc. Rev.* **2018**, *47*, 8349–8402. [CrossRef]
9. Maki-Arvela, P.; Simakova, I.L.; Salmi, T.; Murzin, D.Y. Production of lactic acid/lactates from biomass and their catalytic transformations to commodities. *Chem. Rev.* **2014**, *114*, 1909–1971. [CrossRef]
10. Amaniampong, P.N.; Trinh, Q.T.; De Oliveira Vigier, K.; Dao, D.Q.; Tran, N.H.; Wang, Y.; Sherburne, M.P.; Jerome, F. Synergistic Effect of High-Frequency Ultrasound with Cupric Oxide Catalyst Resulting in a Selectivity Switch in Glucose Oxidation under Argon. *J. Am. Chem. Soc.* **2019**, *141*, 14772–14779. [CrossRef]
11. Ikeda, Y.; Park, E.Y.; Okuda, N. Bioconversion of waste office paper to gluconic acid in a turbine blade reactor by the filamentous fungus Aspergillus niger. *Bioresour. Technol.* **2006**, *97*, 1030–1035. [CrossRef] [PubMed]
12. Li, Y.; Xue, Y.; Cao, Z.; Zhou, T.; Alnadari, F. Characterization of a uronate dehydrogenase from Thermobispora bispora for production of glucaric acid from hemicellulose substrate. *World J. Microbiol. Biotechnol.* **2018**, *34*, 102. [CrossRef] [PubMed]
13. Sheldon, R.A. Green and sustainable manufacture of chemicals from biomass: State of the art. *Green Chem.* **2014**, *16*, 950–963. [CrossRef]
14. Serrano-Ruiz, J.C.; Luque, R.; Sepulveda-Escribano, A. Transformations of biomass-derived platform molecules: From high added-value chemicals to fuels via aqueous-phase processing. *Chem. Soc. Rev.* **2011**, *40*, 5266–5281. [CrossRef]
15. Omri, M.; Pourceau, G.; Becuwe, M.; Wadouachi, A. Improvement of Gold-Catalyzed Oxidation of Free Carbohydrates to Corresponding Aldonates Using Microwaves. *ACS Sustain. Chem. Eng.* **2016**, *4*, 2432–2438. [CrossRef]
16. Samoilova, N.A.; Krayukhina, M.A.; Blagodatskih, I.V.; Vishivannaya, O.V.; Yamskov, I.A. Oxidation of glucose to gluconate on glucose oxidase/nanogold colloidal and heterogeneous catalysts. *Catal. Lett.* **2017**, *147*, 383–390.
17. Wang, W.; Xie, Y.; Zhang, S.; Liu, X.; Zhang, L.; Zhang, B.; Haruta, M.; Huang, J. Highly efficient base-free aerobic oxidation of alcohols over gold nanoparticles supported on ZnO-CuO mixed oxides. *Chin. J. Catal.* **2019**, *40*, 1924–1933. [CrossRef]
18. Khallouk, K.; Solhy, A.; Kherbeche, A.; Dubreucq, E.; Kouisni, L.; Barakat, A. Effective Catalytic Delignification and Fractionation of Lignocellulosic Biomass in Water over $Zn_3V_2O_8$ Mixed Oxide. *Chem. Eng. J.* **2020**, *385*, 123914. [CrossRef]
19. Amaniampong, P.N.; Trinh, Q.T.; Wang, B.; Borgna, A.; Yang, Y.; Mushrif, S.H. Biomass Oxidation: Formyl C-H Bond Activation by the Surface Lattice Oxygen of Regenerative CuO Nanoleaves. *Angew. Chem. Int. Ed.* **2015**, *54*, 8928–8933. [CrossRef]
20. Jia-Xiong, W.U.; Yuan, H.; Zhang, P.; Zhang, H.L.; Yuan-Xin, W.U. Synthesis of Glucuronic Acid by Selective Oxidation of Methyl Glucoside with Active MnO_2 under Microwave. *Chem. Eng. J.* **2012**, *207*, 72–75.
21. Zhou, C.; Xiao, Y.; Xu, S.; Li, J.; Hu, C. γ-Valerolactone Production from Furfural Residue with Formic Acid as the Sole Hydrogen Resource via an Integrated Strategy on Au-Ni/ZrO_2. *Ind. Eng. Chem. Res.* **2020**, *59*, 17228–17238. [CrossRef]
22. Zhou, X.; Li, W.; Mabon, R.; Broadbelt, L.J. A mechanistic model of fast pyrolysis of hemicellulose. *Energy Environ. Sci.* **2018**, *11*, 1240–1260. [CrossRef]
23. Liu, W.J.; Li, W.W.; Jiang, H.; Yu, H.Q. Fates of Chemical Elements in Biomass during Its Pyrolysis. *Chem. Rev.* **2017**, *117*, 6367–6398. [CrossRef] [PubMed]
24. Liu, F.; Huang, K.; Zheng, A.; Xiao, F.-S.; Dai, S. Hydrophobic Solid Acids and Their Catalytic Applications in Green and Sustainable Chemistry. *ACS Catal.* **2017**, *8*, 372–391. [CrossRef]
25. Xu, S.; Wu, Y.; Li, J.; He, T.; Xiao, Y.; Zhou, C.; Hu, C. Directing the Simultaneous Conversion of Hemicellulose and Cellulose in Raw Biomass to Lactic Acid. *ACS Sustain. Chem. Eng.* **2020**, *8*, 4244–4255. [CrossRef]
26. He, T.; Jiang, Z.; Wu, P.; Yi, J.; Li, J.; Hu, C. Fractionation for further conversion: From raw corn stover to lactic acid. *Sci. Rep.* **2016**, *6*, 38623. [CrossRef]

27. Jiang, Z.; Fan, J.; Budarin, V.L.; Macquarrie, D.J.; Gao, Y.; Li, T.; Hu, C.; Clark, J.H. Mechanistic understanding of salt-assisted autocatalytic hydrolysis of cellulose. *Sustain. Energy Fuel.* **2018**, *2*, 936–940. [CrossRef]
28. Jiang, Z.; Yi, J.; Li, J.; He, T.; Hu, C. Promoting Effect of Sodium Chloride on the Solubilization and Depolymerization of Cellulose from Raw Biomass Materials in Water. *ChemSusChem* **2015**, *8*, 1901–1907. [CrossRef]
29. Xu, S.; Xiao, Y.; Zhang, W.; Liao, S.; Yang, R.; Li, J.; Hu, C. Relay catalysis of copper-magnesium catalyst on efficient valorization of glycerol to glycolic acid. *Chem. Eng. J.* **2022**, *428*, 132555. [CrossRef]
30. Xu, S.; Li, J.; Li, J.; Wu, Y.; Xiao, Y.; Hu, C. D-Excess-LaA Production Directly from Biomass by Trivalent Yttrium Species. *iScience* **2019**, *12*, 132–140. [CrossRef]
31. Xu, S.; He, T.; Li, J.; Huang, Z.; Hu, C. Enantioselective synthesis of D-lactic acid via chemocatalysis using MgO: Experimental and molecular-based rationalization of the triose's reactivity and preliminary insights with raw biomass. *Appl. Catal. B Environ.* **2021**, *292*, 120145. [CrossRef]
32. Frisch, M.J.; Trucks, G.W.; Schlegel, H.B.; Scuseria, G.E.; Robb, M.A.; Cheeseman, J.R.; Scalmani, G.; Barone, V.; Mennucci, B.; Petersson, G.A.; et al. *Fox, Gaussian 09 (Revision D.01)*; Gaussian: Wallingford, CT, USA, 2013.
33. Krishnan, R.; Binkley, J.S.; Seeger, R.; Pople, J.A. Self-consistent molecular orbital methods. XX. A basis set for correlated wave functions. *J. Chem. Phys.* **1980**, *72*, 650–654. [CrossRef]
34. Hay, P.J.; Wadt, W.R.; Kahn, L.R. Ab initio effective core potentials for molecular calculations. II. All-electron comparisons and modifications of the procedure. *J. Chem. Phys.* **1978**, *68*, 3059–3066. [CrossRef]
35. Marenich, A.V.; Cramer, C.; Truhlar, D. Performance of SM6, SM8, and SMD on the SAMPL1 Test Set for the Prediction of Small-Molecule Solvation Free Energies. *J. Phys. Chem. B* **2009**, *113*, 4538–4543. [CrossRef] [PubMed]
36. Gonzalez, C.; Schlegel, H.B. An improved algorithm for reaction path following. *J. Chem. Phys.* **1989**, *90*, 2154–2161. [CrossRef]
37. Kresse, G.; Furthmüller, J. Efficiency of ab-initio total energy calculations for metals and semiconductors using a plane-wave basis set. *Comput. Mater. Sci.* **1996**, *6*, 15–50. [CrossRef]
38. Perdew, J.P.; Burke, K.; Ernzerhof, M. Generalized gradient approximation made simple. *Phys. Rev. Lett.* **1996**, *77*, 3865. [CrossRef]
39. Kresse, G.; Joubert, D. From ultrasoft pseudopotentials to the projector augmented-wave method. *Phys. Rev. B* **1999**, *59*, 1758–1775. [CrossRef]
40. Blöchl, P.E. Projector augmented-wave method. *Phys. Rev. B Condens. Matter Mater. Phys.* **1994**, *50*, 17953–17979. [CrossRef]
41. Dudarev, S.L.; Botton, G.A.; Savrasov, S.Y.; Humphreys, C.J.; Sutton, A.P. Electron-energy-loss spectra and the structural stability of nickel oxide: An LSDA+U study. *Phys. Rev. B* **1998**, *57*, 1505–1509. [CrossRef]